Electronic Supplementary Material (ESI) for Nanoscale.

Caged Gold Nanostars: A novel plasmonic nanoplatform with potential theranostic applications

Aidan J Canning [a,b] and Tuan Vo-Dinh [*a,b,c]

[a.] *Department of Biomedical Engineering, Duke University, Durham, NC 27708, USA.*

[b.] *Department of Chemistry, Duke University, Durham, NC 27708, USA*

[c.] *Fitzpatrick Institute for Photonics, Duke University, Durham, NC 27708, USA*

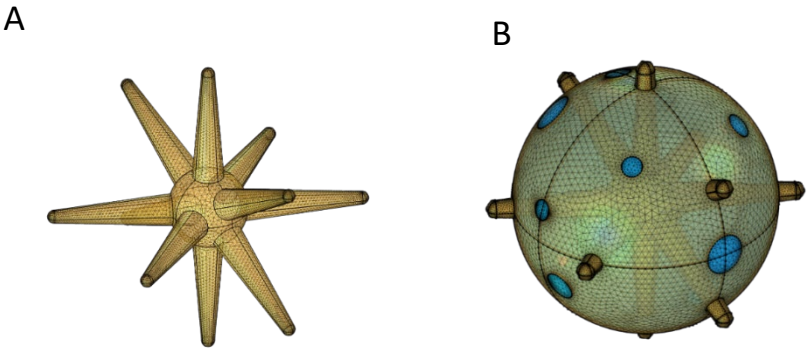

Figure S1. COMSOL models used for nanoparticle simulations. A) COMSOL model of GNS. B) COMSOL model of unsealed C-GNS.

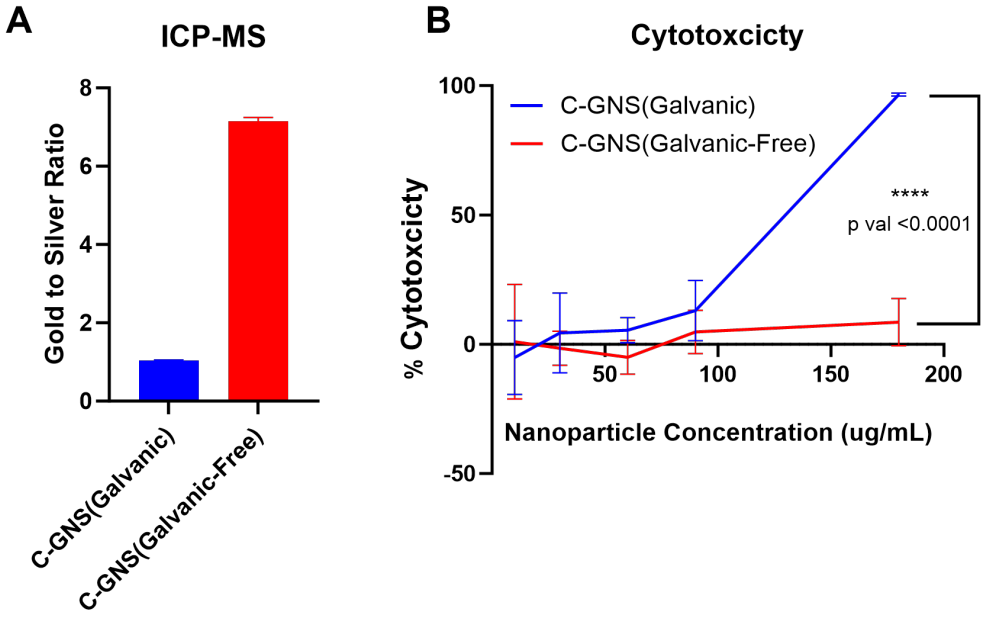

Figure S2. Unsealed C-GNS characterization and cytotoxcicty. A) ICP-MS results of nanoparticle analysis. B) Cytotoxicity study comparing C-GNS particles prepared through different chemical routes.

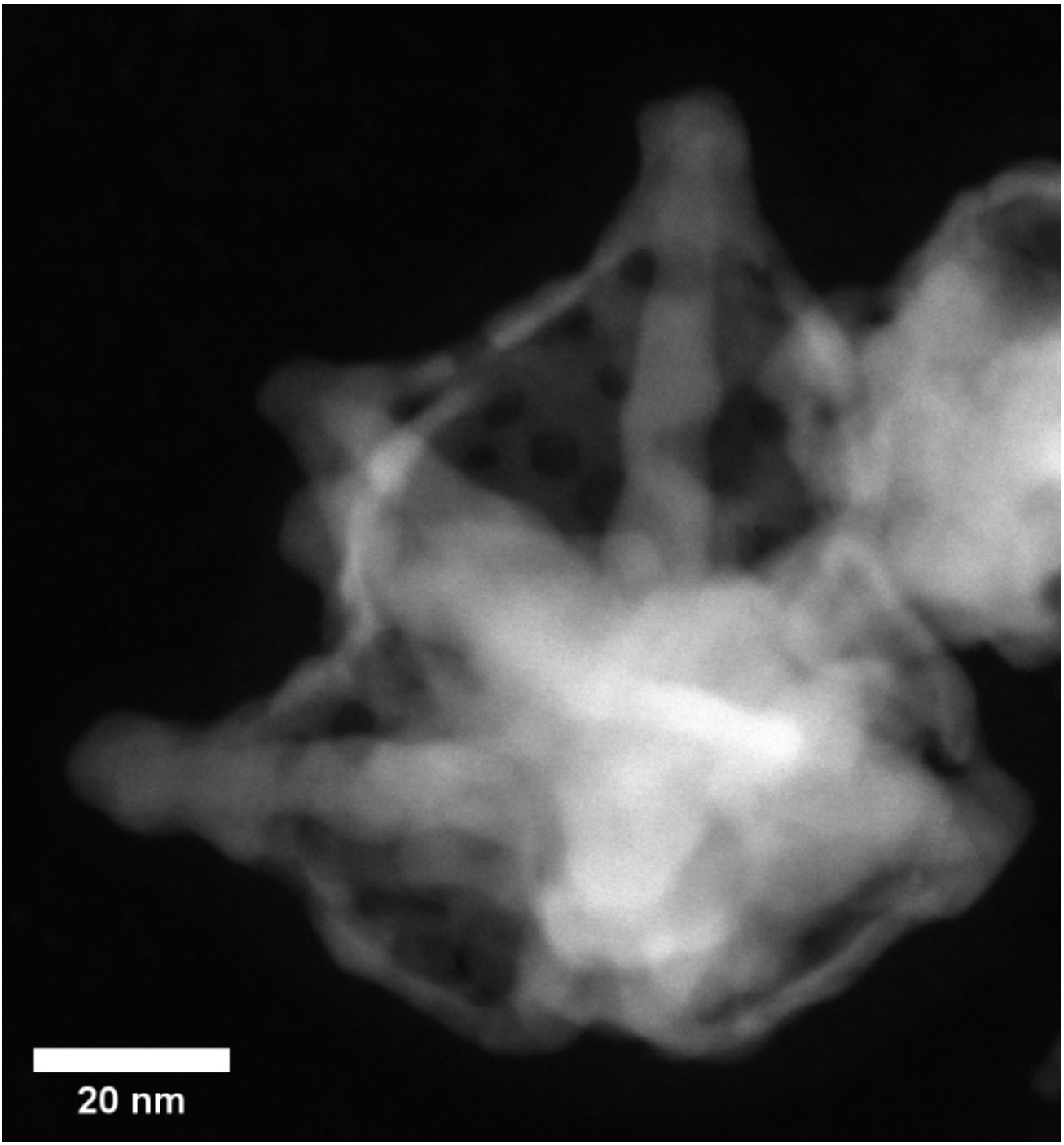

Figure S3. High-resolution STEM image clearly depicting holes in the hollow unsealed C-GNS shell.

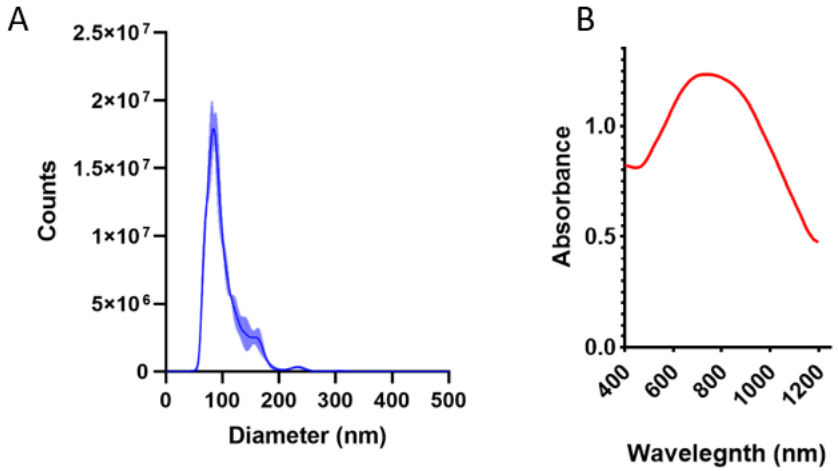

Figure S4. Additional sealed C-GNS particle characterization. A) Nanoparticle tracking analysis of sealed C-GNS particles. B) Absorption Spectra of sealed C-GNS particles.

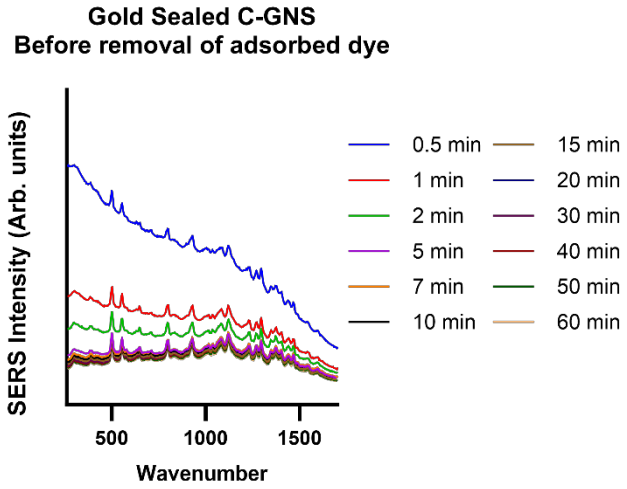

Figure S5. SERS signal over time of sealed C-GNS particles in dilute hydrogen peroxide before the removal of dye adsorbed on the outer surface.

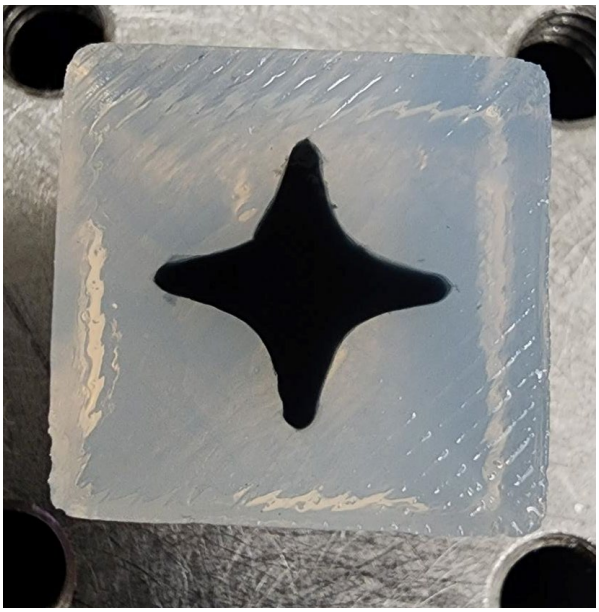

Figure S6. Image of C-GNS phantom.

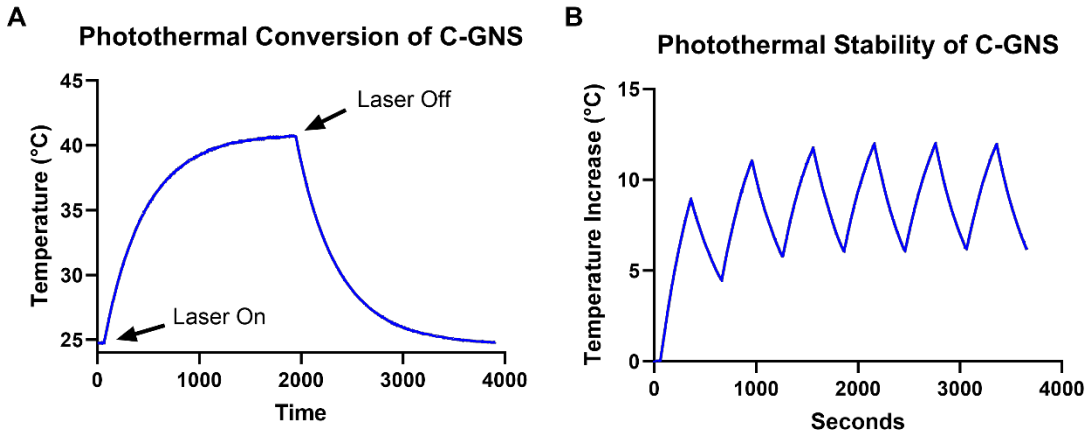

Figure S7. A) Photothermal heating and cooling curve of C-GNS solution used to determine photothermal conversion efficiency. B) Photothermal stability study of C-GNS.

$$\mathrm{CEM3°C} = \sum_{i=1}^{n} t_i * R^{(43-T_i)}, \qquad R(T < 43°C) = \frac{1}{4}, R(T > 43°C) = \frac{1}{2}$$

Equation S1. The formal equation to calculate the cumulative effective minutes at 43°C for hyperthermia treatments.

Methods

Bimetallic Nanostar Synthesis

Surfactant-free gold nanostars were prepared via the method described by Yuan et al. [1] First 12 nm gold spheres were prepared by adding 15 ml 1% citrate solution to 100 mL of 1 mM boiling gold chloride solution. After 30 minutes, the solution was allowed to cool to room temperature and was diluted to a concentration of 10 nM. To prepare a 100 mL solution of 0.1 nM nanostars, 1 mL of seed solution was added to 100 mL of 0.25 mM gold chloride and 100ul of hydrochloric acid. Then rapidly 500ul of 2mM silver nitrate and 500 ul of 0.1 M ascorbic acid. For bimetallic nanostar synthesis, 500 ul of 0.1 M silver nitrate was added to the GNS solution, followed by 100 ul of ammonia hydroxide, as described by Fales et al.[2]

Galvanic Replacement-free C-GNS Preparation

For the gold coating of the bimetallic nanostars, 100 mL of the solution mentioned in the previous step was centrifuged and resuspended in 100 mL solution of 20 mg/mL PVP_{55000}, 17.6 mg/mL ascorbic acid, and 500 uL of NaOH. A syringe pump added 1.5 mL of 5 mM gold chloride solution to the rapidly spinning mixture over 1 hour. After the gold coating was complete, the solution was then centrifuged and resuspended in 10 mL of 55 mg/mL PVP solution.

The concentrated gold-coated bimetallic nanostars were then added to a 50 mL solution of 55 mg/mL PVP and 6% hydrogen peroxide with 300 uL of HCL at 65 °C for 45 minutes to remove the silver from the nanoparticles. After etching, the C-GNS particles were washed several times in water and then in ethanol to remove the insoluble silver chloride which formed during the etching process. Surface-bound PVP was also removed via these ethanol washes. C-GNS particles were then stored in this ethanol solution until further processing.

Galvanic Replacement Preparation of C-GNS

BNS particles were washed and resuspended in 100 mL of 20 mg/mL PVP solution and 300 uL of HCl. 2 mL of Gold chloride was added via a syringe pump for 1 hour.

MTT Assay for Nanoparticle Cytotoxicity

The MTT cytotoxicity kit from abcam ab211091 was used to measure the cytotoxicity of C-GNS particles prepared via galvanic replacement and galvanic replacement-free derived particles. In a 96-well clear

bottom plate, 104 MB49 cells were seeded with 100 uL of DMEM + 10% FBS and incubated overnight. Vary concentrations of C-GNS particles were added to wells and incubated for 24 hours. The nanoparticles were removed, and the assay was performed according to the manufacturer's protocol.

Dye Loading and Sealing of C-GNS

100 mL of 0.1 nM C-GNS particles in ethanol were concentrated to 1 mL and resuspended in ethanol. 1 mg of HITC dye was added to the concentrated nanoparticle solution and mixed overnight. The following day the nanoparticle solution was added to a 100 ml solution of 20 mg/mL PVP. Next, 100 uL of HCl was added, followed by 500 uL of ascorbic acid. After 10 minutes, a syringe pump added 1.5 mL of 5 mM gold chloride solution to the mixture. Sealed C-GNS particles were washed several times in ethanol and incubated in a 20 uM COOH-PEG_{5000}-SH ethanol solution at 50 °C overnight. SERS measures were performed using a 785 nm Wasatch all-in-one laser and spectrometer system. All nanoparticle absorbance spectra were recorded using a Fluorstar Omega spectrometer. All EDS-STEM and HAADF-STEM images were taken using a Talos F200X.

Nanoparticle Tracking Analysis

NTA was performed using a Nanosight S500 by Malvern Panalytical, running version 3.4 of the NTA software. Per software instructions, Particles were diluted until between 10 and 100 particles were visible within the field of view. Three individual runs were averaged to obtain sealed C-GNS data. Nanoparticle concentration data derived from the NTA was used to estimate particle concentrations.

Dye Loading Verification of C-GNS

0.1 nM solutions of sealed and unsealed C-GNS particles suspended in an aqueous 3% hydrogen peroxide solution were prepared. SERS measurements were recorded using a 785 nm Wasatch all-in-one laser and spectrometer system at regular time points.

FEM Simulations

All FEM simulations were performed using the wave optics package within COMSOL Multiphysics 6.0. The simulation domain was spherical and had a radius of 500 nm in all directions. All domains surrounding the nanoparticle and the water domain within the C-GNS structure utilized the optical properties described by Diamon and Masumura.[3] The optical properties of gold described by Johnson and Christy were used for all gold domains making up all nanoparticle morphologies simulated here.[4] The meshing of all simulated particle models was physics-controlled and set to extremely fine.

The base nanostar morphology for all simulated models with a core radius of 15 nm, branch length of 45 nm, and a branch tip diameter of 5 nm. The model of the unsealed C-GNS had holes placed randomly across the surface of the 1 nm thick shell to mimic the morphology seen after peroxide etching. The model used to simulate a sealed C-GNS particle had the outer gold shell thickness increased to 4 nm.

Photothermal Characterization of C-GNS

A quartz optical cuvette was suspended over a stir plate and held in place with an adjustable dual-prong clamp to thermally isolate the sample. Next, 1.5 mL of DI water was added to the cuvette and a small magnetic stir bar to homogenize the solution. The sample was then irradiated with 600 mW at 1064 nm. A hypodermic thermocouple was placed into the solution above the laser level to record the temperature. The sample was heated until equilibrium was reached, at which point the laser was turned off, and the solution was allowed to cool to room temperature. This method was repeated for a C-GNS concentration of 30 ug/mL. Using the cooling curves from both samples, the photothermal conversion efficiency of the C-GNS particles was calculated by the method described in detail by a[5] To calculate photothermal conversion efficiency, the following equations were used:

$$\eta = \frac{hA(T_{\max C-GNS} - T_{amb}) - Q_o}{I(1-10^{-A_\lambda})} \quad (2)$$

$$\tau = \frac{\sum_i m_i C_{pi}}{hA} \quad (3)$$

$$Q_o = hA(T_{solv} - T_{amb}) \quad (4)$$

$$T_{max} - T_{amb} = e^{\frac{-t}{\tau}} \quad (5)$$

Where η is the photothermal conversion efficiency, h is the heat transfer coefficient, A is the sample well surface area, $T_{\max C-GNS}$ is the steady state maximum temperature of C-GNS solution, T_{amb} is the ambient temperature, Q_o is the contribution made by solvent and heating cell, I is the laser power, A_λ is the optical density at 1064 nm, τ is the thermal time constant, m_i is the mass of each component within the cell, C_{pi} is the heat capacity of each component in the cell. T_{solv} is the maximum steady state temperature of water only. The optical density of the C-GNS solution at 1064 nm was 0.527, and the thermal time constants for water only and C-GNS solution were 438.7 and 412.3, respectively. The maximum temperature of the C-GNS solution was 40.7 °C, and the maximum temperature of the water solution was 28.4 °C.

The same experimental setup used for the photothermal conversion efficiency study was used to investigate the photothermal stability of the C-GNS solution. Here, the laser was cycled every 5 minutes for 6 complete cycles.

C-GNS Phantom Preparation

A 3% agarose solution was prepared by adding 3 g of Omnipur agarose to 100 mL of water, bringing the solution to a boil. Once clear, the solution was pipetted into a 3d printed phantom mold. Once the phantom had dried, it was removed from the mold and placed into a container filled with water. Next, a 1.8 mL aliquot of the boiling agarose mixture and pipetted into a 20mL scintillation vial with a stir bar. While mixing, 200 uL of a 2.5 nM C-GNS solution is added to the mixing vial. Once fully mixed, an aliquot of the C-GNS loaded gel is pipetted into a recessed region of the phantom and allowed to solidify.

Live Subject Statement

In this study, all animal studies were performed under a protocol approved by the Institutional Animal Care and Use Committee at Duke University. Duke University's Animal Care and Use program is fully accredited by AAALAC International and registered as a research facility with the US Department of Agriculture in accordance with the Animal Welfare Act and all amendments and holds a Category 1 Assurance with the Public Health Service (through the NIH's Office of Laboratory Animal Welfare). All mice used in this study were B6 albino mice procured from Charles River labs.

Murine Bladder Cancer Model

In this study, female B6 albino mice aged 8-12 weeks were implanted with 250,000 MB49 murine bladder cancer cells on the right-hand flank. Once the tumors had reached a size between 100-200mm^3, mice were eligible for treatment. Animals randomly selected for C-GNS treatment were given a 100uL injection containing 1.5 mg of particles via retroorbital injection. Particle mass verified via ICP-MS. Particles were allowed to circulate in the C-GNS group for 24 hours before further study. Animals were anesthetized using isoflurane via a nose cone for all imaging and photothermal treatment. All animal studies were approved by the Institutional Animal Care and Use Committee of Duke University (protocol number A120-20-06), and all methods were performed following the guidelines and regulations in place.

In Vivo Hyperspectral Imaging

Imaging was performed using a 2x magnification lens with a 5.63 cm working distance for a large field of view capture. A 1 x 4 optical fiber was used to split the 785 nm excitation source to prevent uneven

illumination across the surface of the animal. CRI manufactured the dual-housing liquid crystal tunable filter used for image collection. A Princeton PROEM 512 camera was used to capture hyperspectral images.

Photothermal Therapy

While anesthetized, the tumor regions of animals were subjected to 10 minutes of 1064 nm radiation with a power density of 600 mW/cm^2. Thermocouple measurements were recorded using hypodermic thermocouple probes placed into the tumor center and a TC-08 thermocouple reader by Omega for 9 minutes and 30 seconds of heating. At which point thermocoupoles were removed, and thermal images were captured with a FLIR thermal camera.

1. H. Yuan, C. G. Khoury, H. Hwang, C. M. Wilson, G. A. Grant and T. Vo-Dinh, *Nanotechnology*, 2012, **23**, 075102.
2. A. M. Fales, H. Yuan and T. Vo-Dinh, *The Journal of Physical Chemistry C*, 2014, **118**, 3708-3715.
3. M. Daimon and A. Masumura, *Appl. Opt.*, 2007, **46**, 3811-3820.
4. P. B. Johnson and R. W. Christy, *Physical Review B*, 1972, **6**, 4370-4379.
5. C. Ayala-Orozco, C. Urban, M. W. Knight, A. S. Urban, O. Neumann, S. W. Bishnoi, S. Mukherjee, A. M. Goodman, H. Charron, T. Mitchell, M. Shea, R. Roy, S. Nanda, R. Schiff, N. J. Halas and A. Joshi, *ACS Nano*, 2014, **8**, 6372-6381.